ACS MATERIALS LETTERS

www.acsmaterialsletters.org

Progress in Carbon Cathodic Host Matrices for Lithium−Sulfur Cells: A Meta Analysis

Published as part of ACS Materials Letters special issue "Post-Lithium Battery Materials".

Liam R. Bird, James B. Robinson, and Paul R. Shearing*

Cite This: *ACS Materials Lett.* 2024, 6, 5363−5374

Read Online

ACCESS | Metrics & More | Article Recommendations | Supporting Information

ABSTRACT: **The development of cathodes for lithium−sulfur (Li−S) batteries requires optimizing a variety of interacting and competing variables, with the early technology readiness level (TRL) of Li−S relative to Li-ion batteries presenting researchers with a wide parameter space. Given the interactions between the positive electrode design and the electrolyte, the development of Li−S electrodes requires comprehensive reporting of parameters to enable a comparison of developments. By developing a tool to aggregate synthesis parameters with cell performance, we summarize the frequency with which different components and electrochemical testing conditions are used, including data from 100 articles. Grouping reported capacity data by composite carbon type, C rate, and sulfur content revealed widespread variation in the maximum capacity and rate of degradation. We hope that the tool developed here will provide a facile workflow and promote consistent reporting across the literature, while also pointing toward routes to improve the design of Li−S positive electrodes.**

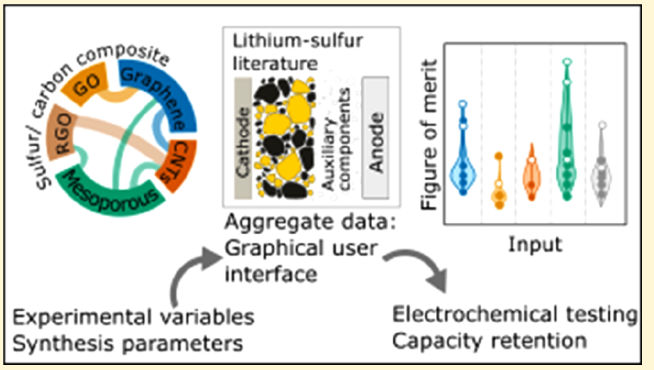

Lithium-sulfur (Li−S) batteries have the potential to play a complementary role to lithium-ion (Li-ion) batteries in enabling the transition to renewably generated electricity.[1] Sulfur's high gravimetric capacity (1675 mAh g^{-1} vs 274 mAh g^{-1} for S_8 and $Li_{0.5}CoO_2$, respectively[2,3]) makes Li−S cells promising for aerospace applications,[1,4,5] and for enabling decarbonization of large payload road freight. Li−S cells store energy using a conversion chemistry mechanism, involving the stepwise reduction of solid S_8 to Li_2S via a series of intermediate lithium polysulfides (PS) (Li_2S_n, $2 \leq n \leq 8$).[2,6] However, the longer chain PS species ($4 \leq n \leq 8$) are soluble in the electrolyte, and their diffusion and electrical isolation from the cathode result in progressive capacity degradation.[1,7] Therefore, a key focus of Li−S research is the development of porous cathodic host matrices to provide and retain electrical interconnection to the electrically insulating active material.[8] Carbon is commonly used as the host matrix due to its electrical conductivity, low cost, and lightweight, which complement the properties of sulfur.

However, Li−S cell performance is sensitive to competing interactions between a range of parameters, including the carbon additive used to supplement the conductivity of the host matrix, binder, electrolyte, and electrochemical testing conditions. Therefore, the evaluation of novel carbon host matrices requires accounting for the influence of these auxiliary components and parameters.

This work aggregates the parameters from 100 research articles detailing 264 separate samples and correlates these experimental inputs with the electrochemical results using a graphical user interface (GUI) (detailed in section SI1 in the Supporting Information). It aims to update the findings of previous meta analyses,[8−10] and to summarize both the values of key parameters used and the frequency with which they are specified in the literature. The meta-analysis focuses on host matrices based on carbon- and/or graphene-related materials (GRMs), with the aim of comparing the effects of parameters related to the host morphology and carbon/sulfur interaction in the absence of dopants and catalysts. There is no unambiguous relationship throughout the surveyed samples between the input parameters and the reported electrochemical performance, indicating the need to consider

Received: August 13, 2024
Revised: November 1, 2024
Accepted: November 1, 2024

https://doi.org/10.1021/acsmaterialslett.4c01646
ACS Materials Lett. 2024, 6, 5363−5374

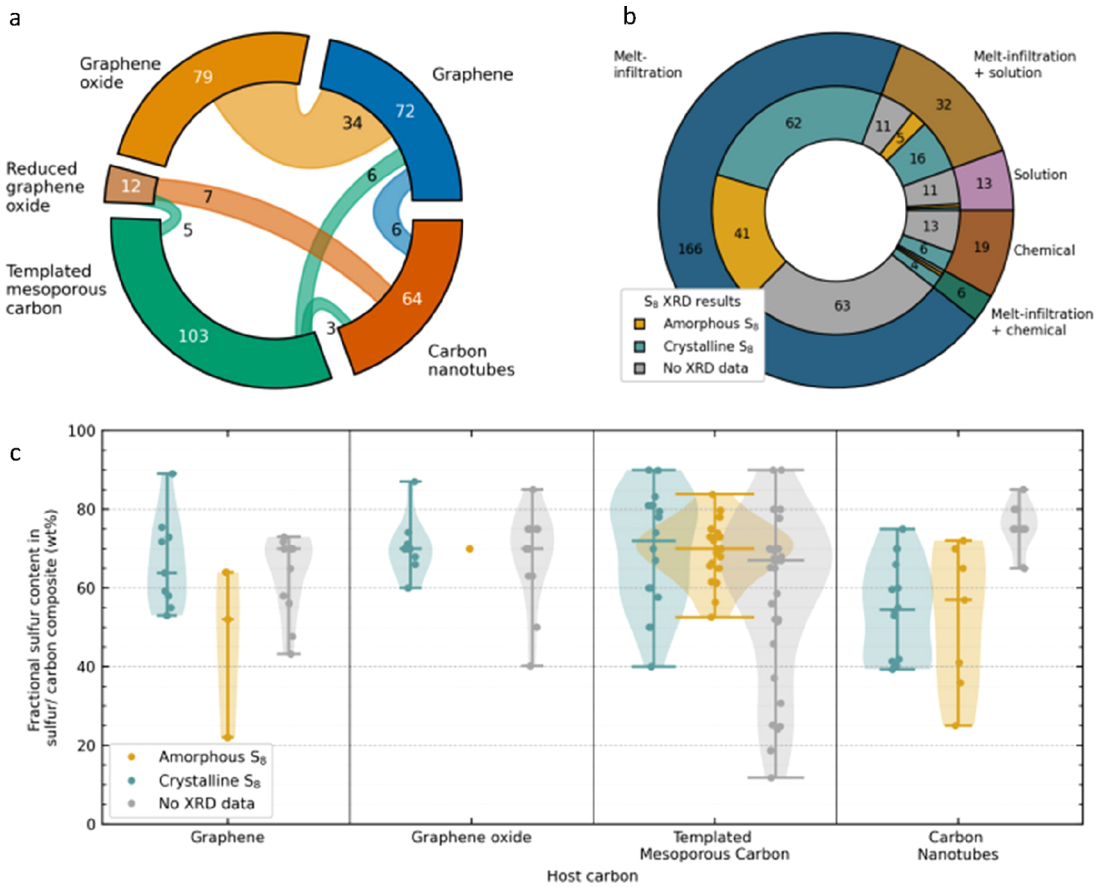

Figure 1. Cathode composite parameters. (a) Frequency of use of different categories of carbon host matrix: values in outer segments show total number of samples using each category in isolation and in mixture; values in chords show the number of samples using a mixture of carbon categories joined by chords. (b) Frequency of use of composite synthesis techniques (outer pie chart), and resulting S_8 crystallinity where reported (inner pie chart). Numerical pie chart labels show the number of samples for one or more samples in the segment. (c) Fractional sulfur loading in sulfur/carbon composite grouped by carbon category and S_8 crystallinity.

interactions between competing parameters when testing candidate host matrices. This analysis highlights the need for consistent utilization and reporting of cell parameters to facilitate evaluation of Li−S cells.

Details of the morphological and electronic properties of carbon host matrices for Li−S cells are reviewed elsewhere,[1,7,9,11,12] while Figure 1a summarizes the distribution of different categories of carbons used in the literature. Templated mesoporous carbons (TMCs) were the most commonly used single category in the articles analyzed: these are amorphous carbon frameworks synthesized by carbonizing a precursor (eg glucose) on a refractory sacrificial template.[13] Renewed interest in Li−S host development was sparked when the work described in ref 14 tailored the morphology of CMK-3 to facilitate PS retention.[14−16] GRMs are also promising candidates, accounting for 53% of the samples included in this meta analysis, with potential for high-throughput synthesis in place of batch-produced TMCs,[17−20] and offering higher electrical conductivity than TMCs. Graphene oxide (GO) and reduced GO (RGO) provide further opportunities to mitigate PS diffusion-related degradation by increasing the binding energy between soluble PS and the cathodic host,[21−23] and decreasing the volume of electrolyte required by improving wetting.[24] By contrast to hierarchical porous structures in TMCs and the sheet-like morphology of GRMs, carbon nanotubes (CNTs) have been investigated as Li−S host matrices due to their high aspect ratio and formation of meshlike, interconnected conductive networks; however, their cost and toxicity[25] limits their compatibility with the advantages of sulfur cathodes. The chords between segments in Figure 1a also highlight the frequency with which carbon categories are used in combination, with complementary morphological and electronic properties: their effectiveness in enabling high capacity realization and retention is compared in later discussion.

Figure 1c shows that the most commonly used fractional sulfur composition is 60−70% across all categories of carbon host, consistent with the content recommended to achieve competitive gravimetric capacity with Li-ion cells specified by the work described in refs 8, 9, and 26 and with the experimental findings to optimize the degree of pore filling by active material while enabling electrolyte ingress/egress.[16,27] The wider range of values reported for TMCs may reflect the greater number of samples (83 vs 30 for CNTs, the second most common single matrix), or a focus on optimizing pore size distribution when developing TMC matrices, leading to reporting of low sulfur content electrodes in the process of optimizing pore filling (see, for example, refs 27−30).

Although 89% of samples with corresponding electrochemical data report the fractional sulfur composition (wt %), only 43% report the areal loading (mg cm^{-2}). The areal loading implicitly reflects the electrode thickness: for example,

https://doi.org/10.1021/acsmaterialslett.4c01646
ACS Materials Lett. 2024, 6, 5363−5374

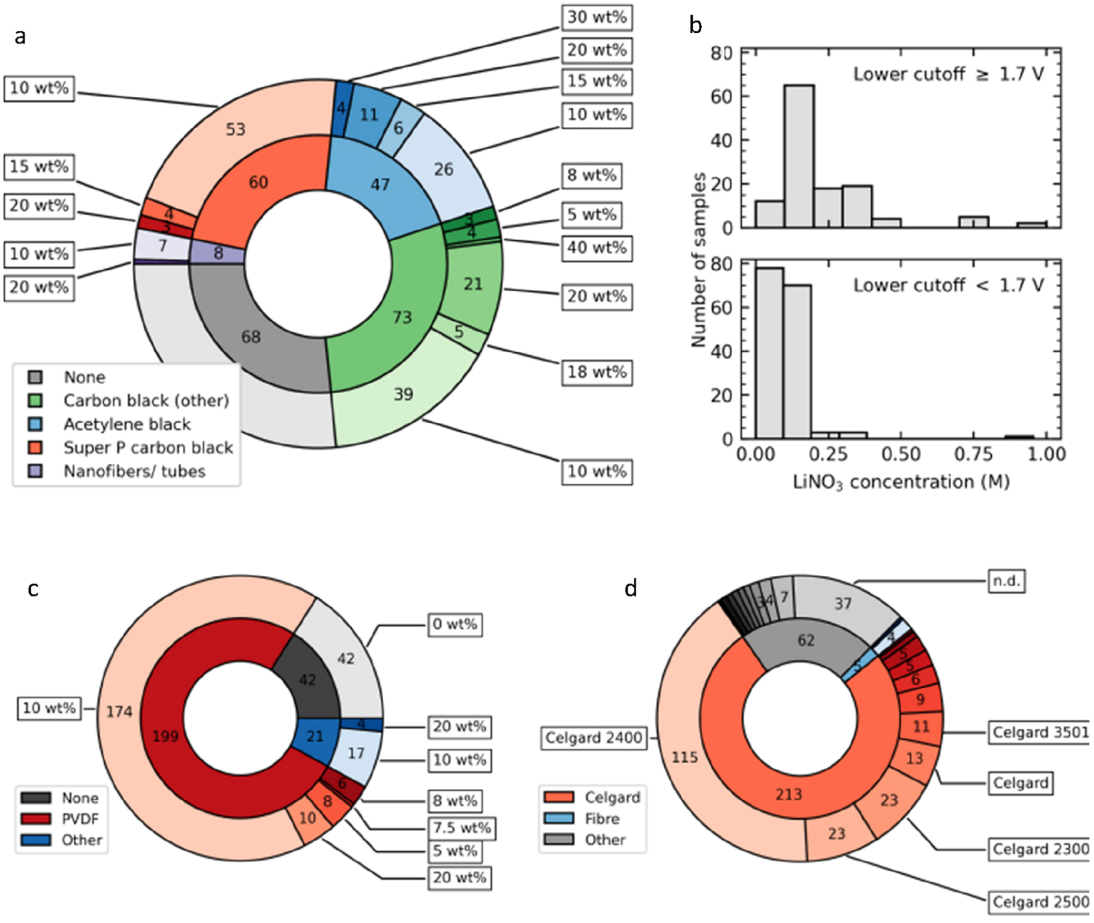

Figure 2. Auxiliary components in Li−S cells. Numerical pie chart labels show number of samples for one or more samples in the segment. (a) Distribution of different categories of conductive carbon additive (inner pie chart) separated by content in the cathode (outer pie chart). (b) Distribution of $LiNO_3$ content in electrolyte (converted to molality where reported in wt %), grouped by lower cutoff voltage used during galvanostatic cycling. (c) Frequency of use of binder materials (inner pie chart) separated by content in the cathode (outer pie chart). (d) Frequency of use of separator materials, with specified materials used by more than 10 samples labeled by name.

Zhao et al.[31] maintained a constant fractional sulfur composition of 56 wt % and compared the rate performance as a function of areal loading. Figure S13 shows that the reported areal loading values are typically consistent with the state-of-the-art (SOTA) values reported in Table S1, and are consistent with the finding that a quantity of 3.5 mg cm^{-2} sulfur balances electrical conductivity with electrode thickness for electrolyte wetting.[24] Due to the interplay of design parameters, an electrode may match the target values for areal sulfur loading shown in Table S1 by means of a low fractional sulfur content in a composite with a high surface area carbon, thereby increasing the necessary electrolyte/sulfur (E/S) ratio, demonstrating the utility of comprehensive reporting in determining optimal configurations.

Figure 1b shows that the most common method of sulfur/carbon composite synthesis is melt infiltration (66% of samples, 83% in combination with other methods). Melt infiltration entails heating a mixture of sulfur and carbon powders to 155 °C, the temperature minimizing the viscosity of molten sulfur,[32] with the aim of producing a uniform interface between the carbon and active material. Alternative methods are denoted as "chemical" (9% of samples) and "solution" (7% of samples). The former involves a solvated precursor ($Na_2S_2O_3$[25,33−37] or Na_2S_x[21,34,37,38]) which is then reduced to form sulfur, frequently using HCl or HCOOH. The latter involves dissolving sulfur in CS_2, either in combination with heating[16,22,31,33,39−46] or without heating,[29,47] or in toluene, similarly in combination with heating[48,49] or without heating.[27] The additional heating steps are typically undertaken at 155 °C to ensure uniform coating, although higher temperatures may be used to remove excess sulfur agglomerates from the carbon surface that has not been imbibed by the porous structure.[28] The prevalence of melt infiltration may be due to the facile control over fractional sulfur content provided by mixing powders and the requirement for no additional chemicals, including those required for solution infiltration, which are toxic.

The work reported in ref 14 demonstrated the efficacy of melt infiltration via the respective presence and absence of crystalline S_8 XRD peaks from composites heated to 145 and 155 °C, with the latter having a higher initial capacity (1005 vs ca. 780 mAh g^{-1}, respectively). The inner pie chart of Figure 1b therefore shows the number of samples qualitatively exhibiting S_8 XRD peaks (determined qualitatively where spectra were reported) for each synthesis method. However, 59% of available XRD spectra for melt-infiltrated composites show crystalline S_8 peaks. The discrepancy with ref 14 may be attributable to differences in fractional sulfur content and carbon surface morphology: Figure 1c shows the association between observation of crystalline S_8, fractional content, and

https://doi.org/10.1021/acsmaterialslett.4c01646
ACS Materials Lett. 2024, 6, 5363−5374

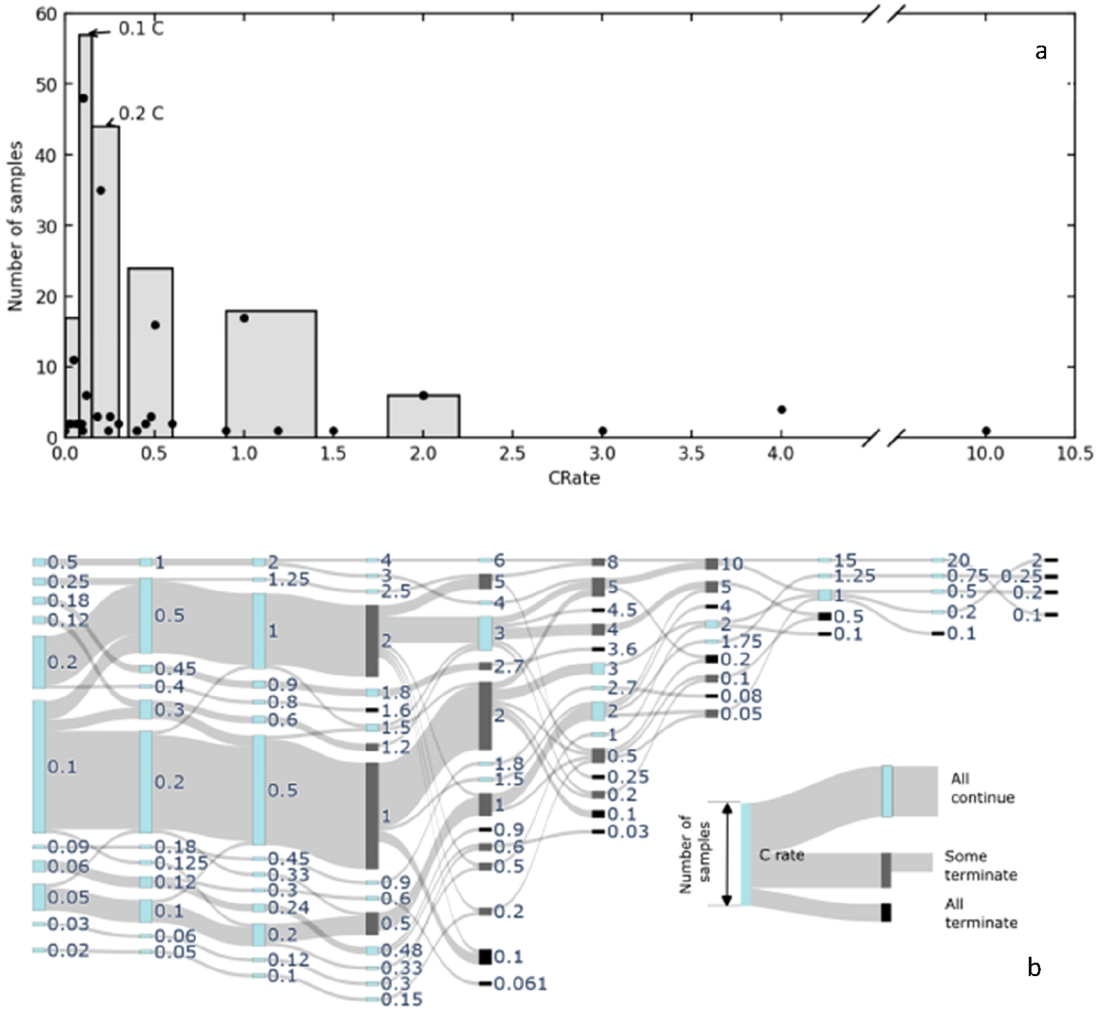

Figure 3. Galvanostatic cycling conditions. (a) Frequency of use of constant C rates, showing unique rates with points and summarizing groups of similar C rates in bars. (b) Rate capability testing protocols, showing the order of different rates (left to right); the width of the bar is proportional to the number of samples following each protocol (see inset legend).

host carbon category, and Figure S14 shows fractional sulfur content grouped by composite synthesis method. Although the median fractional content is marginally higher where crystalline S_8 is observed for all carbons, the distributions strongly overlap. This absence of a causal relationship between experimental parameters and composite properties hinders direct comparison between reports, possibly explaining the absence of sulfur/carbon composite XRD characterization from 44% of the samples.

Figure 2a shows that 73% of samples in this meta analysis use a supplemental carbon additive in addition to the carbon host matrix, with 65% using 10 wt % carbon black (of which 34% specify Super P carbon black). It is likely that the type and quantity of conductive carbon additives used in Li−S cathodes is inherited from Li-ion cathode development, where they are used to support inherently low conductivity active materials including Li_xCoO_2 (10^{-3} S cm^{-1})[50] and $LiFePO_4$ (10^{-9} S cm^{-1}).[51,52] The carbon additive content must be sufficient to provide a continuous conductive network but avoid mechanical instability due to aggregation of carbon additive islands at higher loadings.[53,54] High surface area carbon additives may result in a capacitive layer buffers the potential drop at the electrode/electrolyte interface and helps mitigate self-discharge.[55] However, while the total contribution of carbon to the mass of a pouch cell is estimated[1] at 5.48% (using an E/S ratio of 2 μL mg^{-1}), the high surface area and tortuosity contributed by low mass-density additives may indirectly contribute to decreased cell-level gravimetric capacity by requiring additional electrolyte to contact this interface.[56]

As shown in Figure 2c, the majority of samples included in this meta analysis use polyvinylidene fluoride (PVDF) binder (77%), with 73% using a binder content (of any type of binder) of 10 wt %: this is consistent with a literature review conducted by Lacey et al.[57] in 2014, who found that 81% of 79 Li−S papers used PVDF binder. The electrode slurry solvent used in all instances of PVDF binder identified during this meta analysis was *n*-methyl-2-pyrrolidone (NMP). An additional 28 samples used alternative binders, including LA132,[58] LA133,[59] styrene butadiene rubber (SBR), and sodium carboxymethylcellulose (CMC),[60] or Selvol 425 PVA,[61] while 47 samples used no binder, because the electrode consisted of freestanding foam, fibrous mats, or similar.[27,31,33,62,63]

The dominant use of 10 wt % binder is consistent with a feasibility study[24] suggesting that a binder content of at least 10 wt % is necessary to prevent delamination of Li−S electrodes with >7 mg cm^{-2} sulfur (compare targets in Table S1), other studies assume a binder content of 5 wt % when

https://doi.org/10.1021/acsmaterialslett.4c01646
ACS Materials Lett. 2024, 6, 5363−5374

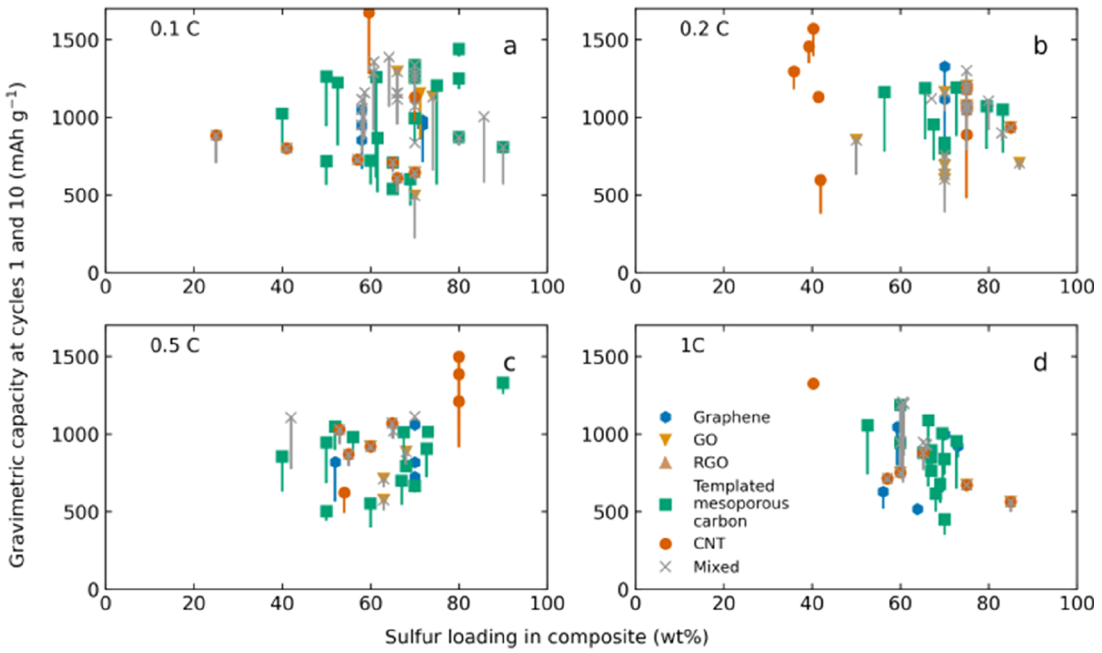

Figure 4. Capacity at the first and 10th cycle (top and bottom of error bars, respectively) with samples grouped by host matrix carbon and C rate ((a) 0.1 C, (b) 0.2 C, (c) 0.5 C, and (d) 1 C).

optimizing other parameters.[4,26] Acknowledging the focus of this meta analysis on host matrix optimization, the widespread use of PVDF reflects its standard use in Li-ion electrodes,[57] because it is electrochemically inert with respect to $LiPF_6$ electrolyte salt[64] and thermochemically stable at standard operating temperatures.[65] However, alternative binders present opportunities for improving Li−S capacity retention through chemisorption/physisorption of soluble PS species using functional groups, by contrast to PVDF where the F atoms provide no permanent dipole due to steric hindance.[66−68] Further benefits are associated with structural differences: the swelling interaction of NMP-dissolved PVDF with Li−S electrolytes may hinder Li^+ ion transport through microporous carbon channels,[57] while bridge-like binder morphologies can be achieved with CMC which retain interconnected porous channels and are resilient to active material redistribution.[69] The use of alternative binders to PVDF also provides opportunities for avoiding the use of toxic NMP solvent, and avoids the release of hydrofluoric acid or perfluoroalkyl substances (PFAS) during possible recycling routes for Li−S batteries involving hydrolysis and pyrolysis;[70] however, the nature of disposal and recycling routes for Li−S batteries is likely to be determined by the use of lithium-metal anodes or their alternatives.

Since this meta analysis focuses on articles seeking to optimize the carbon host matrix, Figures 2d and S15 show that the separator and electrolyte selected are more consistent than other parameters discussed here. In addition, 80% of samples used polypropylene (PP) separators, 95% of which specify Celgard. Although differences in surface treatments may introduce differences in the separator interaction with the electrolyte and dissolved active material, separators with similar composition and thickness are likely to require similar volumes of electrolyte (by contrast to thicker glass fiber separators, used in only five samples). Therefore, separator use may be a useful indicator in the absence of reporting the volume of electrolyte or E/S ratio. Notably, 14% of samples did not report the type of separator used limiting the opportunity for reproduction of the studies.

Figure S15 shows 86% of samples in the meta analysis use 1:1 v/v 1,3-dioxolane and 1,2-dimethoxyethane (DOL:DME) as the electrolyte solvent,[2,32] with 88% of samples using 1 M LiTFSI electrolyte salt. 73% of samples also used $LiNO_3$ as an additive with the aim of forming a stable passivating layer incorporating lithium sulfates on the lithium anode to mitigate the PS shuttle effect,[71,72] in addition to providing Li^+ ions for electrolyte conductivity.[73] However, $LiNO_3$ undergoes irreversible reduction at 1.7−1.8 V vs lithium;[74] therefore, discharging to voltages below 1.7 V may result in additional discharge capacity during the first cycle due to the consumption of $LiNO_3$, followed by irreversible capacity degradation due to formation of Li_2S as a precipitate on the lithium anode surface.[74,75] However, Figure 2b shows that 50 of the 95 samples with lower cutoff voltages below 1.7 V used no $LiNO_3$, compared to 7 of 117 samples using cutoff voltages of ≥1.7 V, with the majority of cells using low cutoff voltages (88 of 95) using <0.1 M $LiNO_3$, possibly mitigating the effect on irreversible capacity in these samples. In addition, the low gassing temperature of $LiNO_3$ poses challenges to the widerspread commercialization of Li−S cells making it incompatible with transportation safety requirements.[76,77] Consequently, its use may be limited in higher technology readiness level (TRL) studies, requiring the use of different electrolyte solvents with corresponding adjustment to the stable voltage range.

The frequency of use of constant C rates for galvanostatic cycling is shown in Figure 3a, dominated by testing at 0.1 C (33%), and 0.2 C (26%). This is consistent with the target of ca. 0.2 C used for cycle life targets (Table S1). Notably, the current density for 0.1 C for Li−S cells (0.167 mA g^{-1}) corresponds to ∼0.6 C testing of Li-ion cells with $Li_{0.5}CoO_2$ cathodes with a theoretical capacity of 274 mAh g^{-1}, hence, the apparent lower target rates than for Li-ion cells.[78] However, the use of C rates of <0.5 C may result in high

https://doi.org/10.1021/acsmaterialslett.4c01646
ACS Materials Lett. 2024, 6, 5363−5374

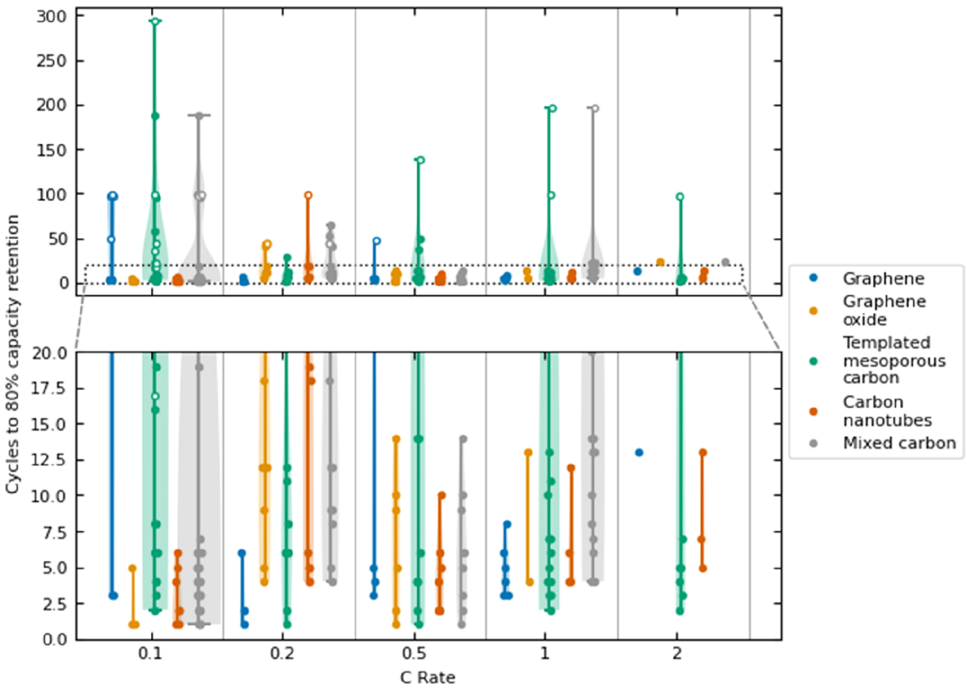

Figure 5. Number of cycles undergone before the capacity decreases to 80% of the maximum reported capacity, grouped by C rate and carbon host type. Filled markers indicate cycle at which 80% of maximum capacity was reached; unfilled markers indicate total number of cycles reported where >80% of capacity was retained throughout the range reported. Lower plot shows an expanded view of the region depicted in the gray dashed box in the upper plot.

initial capacities but lower reversibility in Li−S cells: higher charging currents mitigate the shuttle of PS and corresponding parasitic electron transfer processes,[79] and limits the accumulation[80] of irreversibly deposited Li_2S. Additionally, of the total 419 cycling results for the 224 samples, 22 reported the use of slower formation cycles before the onset of a higher C rate, which enable the conversion and redistribution of active material on the carbon interface while minimizing kinetic limitations, which may apply at higher rates. These were most commonly used for ≤2 cycles (17 of 22), and the current used commonly corresponded to ∼10% (8 of 22) or ∼20% (7 of 22) of the higher continuous C rate.

In addition, 70 samples reported rate performance testing results, entailing cycling cells at a sequence of progressively higher C rates, frequently terminated by resuming the original low C rate. This demonstrates capacity degradation/retention mechanisms, including active material becoming inaccessible at high C rates due to pore blocking by preferential deposition of Li_2S at the electrode surface. Moreover, returning to a low C rate indicates whether this capacity can be recovered, given a longer duration for soluble species to percolate the electrode. Figure 3b shows the stepwise sequences (left to right), with the path width corresponding to the number of samples. To enable this grouping, the number of cycles undertaken at each step is not considered: while some tests use the same number of cycles at every step, some use more cycles in the first or terminal step. The variety in protocols shown in Figure 3b frustrates the comparison of the effect of cycling history on capacity, including effects of cumulative precipitation or degradation. It is unclear whether it is more representative of likely operating conditions to change abruptly from the maximum rate to a lower rate, and the consequences for recovering electrochemical utilization of material precipitated at high C rates. Additionally, by contrast to constant rate test, 92% of rate performance tests meet or exceed 1 C. Similar to the unclear effect of slow initial formation cycles discussed above, the diversity of cycling histories during rate performance testing makes it impossible to evaluate whether incremental increases in C rate enable redistribution and reversible utilization of a greater proportion of the active material when C rates of ≥1 C are attained than if a rate of ≥1 C is used throughout the cycling life.

As the most commonly reported parameter available, the fractional sulfur content is used to compare the capacity attained by samples undergoing constant rate cycling, grouped by host matrix category and C rate. For each sample the top and bottom of the "error bars" in Figure 4 show the first and 10th cycle capacity, respectively, with the aim of reflecting the maximum and stable capacity attained. At 0.1 and 0.2 C, for which more data was available, the attained capacities are not stratified by host matrix material, with no host matrix unambiguously outperforming the others. At 0.1 C, there is an overall negative correlation between sulfur loading and capacity for all groups of materials: this is consistent with the information given in ref 16, which showed that the total sulfur utilization was limited by the interface available for electrochemical between sulfur and the conductive host matrix, and adding additional sulfur increased the total capacity of the cell while the gravimetric capacity remained similar. The reportgiven in ref 81 demonstrated this effect using series of tomograms of cells with different initial sulfur morphologies, finding that larger initial sulfur particles (likely to be characteristic of higher sulfur content composites) resulted in slower rate capability, but they did function as reservoirs to buffer capacity degradation due to inventory loss. However, this relationship is not upheld by the lower extent of the "error bars" in Figure 4, which show no unambiguous correlation between capacity retained after 10 cycles and higher sulfur

https://doi.org/10.1021/acsmaterialslett.4c01646
ACS Materials Lett. 2024, 6, 5363−5374

content in composites. Furthermore, Figure 4b shows results for cells using GO host matrices and similar sulfur content of 41 wt %, but attaining initial (10th cycle) capacities of 1570 mAh/g (1395 mAh/g) and 597 mAh/g (390 mAh/g), respectively, highlighting the influence of other parameters on capacity attained and retained by electrodes utilizing the same carbon host matrix, the same sulfur content in the composite, and the same C rate.

Although the 10th cycle was used for comparison in Figure 4, this is an arbitrary choice and different rates of capacity decline and stabilization make selection of a comparable cycle number difficult. However, availability of capacity data at every cycle using the numerical data inference process demonstrated in section SI1 in the Supporting Information makes it possible to define a figure of merit (FOM)[10] based on the U.S. Advanced Battery Consortium (USABC) definition of the end of life for rechargeable automotive batteries, namely degradation to 80% of the initial capacity.[82] Cells retaining ≥80% of their initial capacity for more cycles are deemed to perform better by using this FOM. Figure 5 shows the number of cycles undergone between the maximum capacity and degradation to 80% of this value, with unfilled markers showing the total number of cycles reported where a sample retained >80% of its initial capacity throughout the reported range.

86% of the samples in Figure 5 decline to ≤80% of their maximum capacity within 20 cycles, reflecting the typical initial irreversible capacity loss characteristic of Li−S cells. Outliers retaining ≥80% of their maximum capacity for more than 100 cycles are reported, particularly at lower C rates; however, this may be associated with "survivorship bias" where cells that are competitive with the SOTA at high C rates report results for a range of constant rates, while other cells reported to be competitive with the SOTA at low C rates may suffer unreported degradation at higher rates. Additionally, the data point showing 300 cycles while retaining ≥80% of the maximum capacity at 0.1 C corresponds to a sample with a modest absolute capacity[83] (ca. 600 mAh g^{-1} throughout), highlighting the need to balance active material utilization with long-term capacity retention. Although more data are available for lower C rates, there is no unambiguous link between carbon host matrix, C rate, and capacity retention, making it difficult to establish relationships between carbon properties under investigation and their effect on electrochemical performance.

Table 1 summarizes the parameters that were not universally included in articles included in the meta analysis. While more frequent reporting would enable the relative influence of each parameter to be established, the lack of established measurands for these infrequently reported parameters makes comparison with existing studies difficult and therefore compounds the lack of incentive to report them. For example, "high electrical conductivity" is frequently cited as motivation for developing carbon host matrices, with the aim of facilitating faster electrical kinetics and lower overpotential, however electrochemical reactions are also limited by the rate of Li^+ ion diffusion.[84] However, where conductivity was reported by articles in this meta-analysis, the measurand was variously the host carbon in isolation,[14,21,37,47,85−89] the sulfur/carbon composite,[14,15,21,41,47,87] or the electrode incorporating a polymer binder and additional conductive additive.[33] Similarly, the surface area and pore size distribution were variously reported for either the host matrix in isolation,[16,25,27,28,37,45,59,61−63,83,85−87,89−111] and/or the sulfur/carbon composite.[14,15,29−31,41,43,58,112−118] Surface area was universally calculated using the multipoint Brunauer−Emmett−Teller (BET) equation: although useful for consistent comparison, the BET equation assumes monolayer N_2 absorption and is therefore unsuitable for determining micropore/nanopore content.[119] Additionally, where reported, the pore size distributions were variously calculated using the Barrett−Joyner−Halenda (BJH) equation,[14,25,28,37,83,85,90,105,107,108,111] with some studies using the Horvath−Kawazoe (HK) equation for micropore determination,[83,85,107] or using density functional theory (DFT) methods.[27,45,92,94,98,101,103,109]

Voluntary checklists of key parameters to report for evaluating cell performance have been compiled by journals including *ACS Energy Letters*,[120] *Joule*,[121] and *Journal of Power Sources*.[122] These include widely reported variables such as carbon type and content, in addition to infrequently reported values including the E/S and negative/positive (N/P) ratios: no examples of the latter were found during this meta analysis, but it is nonetheless included as a target metric by ref 56. Electrode thickness is included as a recommended reported parameter by two sets of guidelines;[121,122] however, a potential additional parameter may be the solid content of electrode slurries. Although 75% of samples in this meta analysis reported using NMP as the slurry solvent, no examples of the quantity added or slurry viscosity were found, which empirically influence the homogeneity and mechanical properties of electrodes. These voluntary guidelines may contribute to more consistent and comprehensive reporting; these checklists were published between 2020 and 2021 while this meta analysis covers reports published to 2023, and these checklists have not yet been universally adopted.

This review summarizes the key approaches to carbon-based host matrix development for Li−S cathodes, in addition to the accompanying electrode parameters and conditions used for electrochemical testing. By aggregating data from 100 articles, this work demonstrates the variation in the mass loading and composition of the active material and auxiliary constituents in Li−S electrodes and the frequency with which different types and combinations of cell components are used and/or reported in articles. The diversity of parameter combinations is reflected by the wide variation in the maximum and retained galvanostatic cycling capacity, with little correlation between commonly reported parameters and electrochemical performance. Standardised testing conditions, including C rates and E/S ratios, are likely to be driven by the establishment of

Table 1. Number of Articles and Corresponding Percentage of Samples Included in Meta Analysis with Data for Infrequently Reported Parameters[a]

parameter	reporting frequency (% samples)	reporting frequency (number of articles)
carbon/composite surface area	57	61
sulfur areal loading (mg cm^{-2})	44	48
pore volume/size distribution	41	45
electrolyte content	25	44
conductivity	13	16
electrode thickness	11	14

[a]For a total of 100 articles.

https://doi.org/10.1021/acsmaterialslett.4c01646
ACS Materials Lett. 2024, 6, 5363−5374

commercial targets in the long term, while in the short term journal publication recommendations[120−122] may encourage more consistent reporting of cell metrics. Future developments in Li−S pouch cells and solid state electrolytes introduce additional interacting variables, including pressure, further strengthening the motivation for consistent parameter reporting to ensure valid evaluation. There are also opportunities for systematic evaluation of the effects of parameters including binder and conductive additive content which have been inherited from Li-ion cells rather than being optimized for Li−S cell chemistry. The GUI developed for this work, accessible via the link provided in the Supporting Information, is designed to facilitate the future expansion of this database with consistent data-entry methods. This analysis highlights the need for consistent benchmarking to elucidate the most influential parameters determining Li−S cell performance and identify the most impactful focus of future research efforts.

■ ASSOCIATED CONTENT

Supporting Information

The Supporting Information is available free of charge at https://pubs.acs.org/doi/10.1021/acsmaterialslett.4c01646.

Graphical user interface example and implementation (SI1); supplementary results figures showing data from main text grouped by alternative variables (SI2); reported attained and target values for cell-level parameters for lithium−sulfur cells collected from the literature (SI3); full list of articles included in meta analysis (SI4) (PDF)

■ AUTHOR INFORMATION

Corresponding Author

Paul R. Shearing − *ZERO Institute, University of Oxford, Oxford OX2 0ES, United Kingdom; The Faraday Institution, Didcot OX11 0RA, United Kingdom;* orcid.org/0000-0002-1387-9531; Email: paul.shearing@eng.ox.ac.uk

Authors

Liam R. Bird − *ZERO Institute, University of Oxford, Oxford OX2 0ES, United Kingdom; The Faraday Institution, Didcot OX11 0RA, United Kingdom*

James B. Robinson − *Advanced Propulsion Lab, University College London, London E20 2AE, United Kingdom; Electrochemical Innovation Lab, University College London, London WC1E 7JE, United Kingdom; The Faraday Institution, Didcot OX11 0RA, United Kingdom;* orcid.org/0000-0002-6509-7769

Complete contact information is available at: https://pubs.acs.org/10.1021/acsmaterialslett.4c01646

Notes

The authors declare no competing financial interest.

■ ACKNOWLEDGMENTS

The authors acknowledge the support of The Faraday Institution's LiSTAR Programme (No. FIRG058). PRS was supported by the Department of Science, Innovation and Technology (DSIT) and the Royal Academy of Engineering under the Chair in Emerging Technologies Programme (No. CiET1718/59).

■ REFERENCES

(1) Robinson, J. B.; Xi, K.; Kumar, R. V.; Ferrari, A. C.; Au, H.; Titirici, M.-M.; Parra-Puerto, A.; Kucernak, A.; Fitch, S. D. S.; Garcia-Araez, N.; Brown, Z. L.; Pasta, M.; Furness, L.; Kibler, A. J.; Walsh, D. A.; Johnson, L. R.; Holc, C.; Newton, G. N.; Champness, N. R.; Markoulidis, F.; Crean, C.; Slade, R. C. T.; Andritsos, E. I.; Cai, Q.; Babar, S.; Zhang, T.; Lekakou, C.; Kulkarni, N.; Rettie, A. J. E.; Jervis, R.; Cornish, M.; Marinescu, M.; Offer, G.; Li, Z.; Bird, L.; Grey, C. P.; Chhowalla, M.; Lecce, D. D.; Owen, R. E.; Miller, T. S.; Brett, D. J. L.; Liatard, S.; Ainsworth, D.; Shearing, P. R. 2021 Roadmap on Lithium Sulfur Batteries. *J. Phys. Energy* **2021**, *3*, No. 031501.

(2) Akridge, J. Li/S Fundamental Chemistry and Application to High-Performance Rechargeable Batteries. *Solid State Ionics* **2004**, *175*, 243−245.

(3) Mizushima, K.; Jones, P. C.; Wiseman, P. J.; Goodenough, J. B. LixCoO2 (0 < x<-1): A New Cathode Material for Batteries of High Energy Density. *Mater. Res. Bull.* **1980**, *15*, 783−789.

(4) Dörfler, S.; Walus, S.; Locke, J.; Fotouhi, A.; Auger, D. J.; Shateri, N.; Abendroth, T.; Härtel, P.; Althues, H.; Kaskel, S. Recent Progress and Emerging Application Areas for Lithium−Sulfur Battery Technology. *Energy Technol.* **2021**, *9*, No. 2000694.

(5) Ellerington, I. *Faraday Report 2020. High-Energy Battery Technologies*; Faraday Institution, 2020. Available via the Internet at: https://web.archive.org/web/20240627164559/https://faraday.ac.uk/wp-content/uploads/2020/01/High-Energy-battery-technologies-FINAL.pdf (accessed June 27, 2024).

(6) Kumaresan, K.; Mikhaylik, Y.; White, R. E. A Mathematical Model for a Lithium−Sulfur Cell. *J. Electrochem. Soc.* **2008**, *155*, A576.

(7) Seh, Z. W.; Sun, Y.; Zhang, Q.; Cui, Y. Designing High-Energy Lithium−Sulfur Batteries. *Chem. Soc. Rev.* **2016**, *45*, 5605−5634.

(8) Hagen, M.; Hanselmann, D.; Ahlbrecht, K.; Maça, R.; Gerber, D.; Tübke, J. Lithium−Sulfur Cells: The Gap between the State-of-the-Art and the Requirements for High Energy Battery Cells. *Adv. Energy Mater.* **2015**, *5*, No. 1401986.

(9) Chung, S.; Chang, C.; Manthiram, A. Progress on the Critical Parameters for Lithium−Sulfur Batteries to Be Practically Viable. *Adv. Funct. Mater.* **2018**, *28*, No. 1801188.

(10) Kilic, A.; Odabaşı, Ç.; Yildirim, R.; Eroglu, D. Assessment of Critical Materials and Cell Design Factors for High Performance Lithium-Sulfur Batteries Using Machine Learning. *Chem. Eng. J.* **2020**, *390*, No. 124117.

(11) Evers, S.; Nazar, L. F. New Approaches for High Energy Density Lithium−Sulfur Battery Cathodes. *Acc. Chem. Res.* **2013**, *46*, 1135−1143.

(12) Chadha, U.; Bhardwaj, P.; Padmanaban, S.; Suneel, R. M.; Milton, K.; Subair, N.; Pandey, A.; Khanna, M.; Srivastava, D.; Mathew, R. M.; Selvaraj, S. K.; Banavoth, M.; Sonar, P.; Badoni, B.; Rao, N. S.; Kumar, S. G.; Ray, A. K.; Kumar, A. Review—Contemporary Progresses in Carbon-Based Electrode Material in Li-S Batteries. *J. Electrochem. Soc.* **2022**, *169*, No. 020530.

(13) Ryoo, R.; Joo, S. H.; Jun, S. Synthesis of Highly Ordered Carbon Molecular Sieves via Template-Mediated Structural Transformation. *J. Phys. Chem. B* **1999**, *103*, 7743−7746.

(14) Ji, X.; Lee, K. T.; Nazar, L. F. A Highly Ordered Nanostructured Carbon−Sulphur Cathode for Lithium−Sulphur Batteries. *Nat. Mater.* **2009**, *8*, 500−506.

(15) Ji, X.; Evers, S.; Black, R.; Nazar, L. F. Stabilizing Lithium−Sulphur Cathodes Using Polysulphide Reservoirs. *Nat. Commun.* **2011**, *2*, 325.

(16) Li, X.; Cao, Y.; Qi, W.; Saraf, L. V.; Xiao, J.; Nie, Z.; Mietek, J.; Zhang, J.-G.; Schwenzer, B.; Liu, J. Optimization of Mesoporous Carbon Structures for Lithium−Sulfur Battery Applications. *J. Mater. Chem.* **2011**, *21*, 16603.

(17) Backes, C.; Abdelkader, A. M.; Alonso, C.; Andrieux-Ledier, A.; Arenal, R.; Azpeitia, J.; Balakrishnan, N.; Banszerus, L.; Barjon, J.; Bartali, R.; Bellani, S.; Berger, C.; Berger, R.; Ortega, M. M. B.; Bernard, C.; Beton, P. H.; Beyer, A.; Bianco, A.; Bøggild, P.; Bonaccorso, F.; Barin, G. B.; Botas, C.; Bueno, R. A.; Carriazo, D.; Castellanos-Gomez, A.; Christian, M.; Ciesielski, A.; Ciuk, T.; Cole,

M. T.; Coleman, J.; Coletti, C.; Crema, L.; Cun, H.; Dasler, D.; De Fazio, D.; Díez, N.; Drieschner, S.; Duesberg, G. S.; Fasel, R.; Feng, X.; Fina, A.; Forti, S.; Galiotis, C.; Garberoglio, G.; García, J. M.; Garrido, J. A.; Gibertini, M.; Gölzhäuser, A.; Gómez, J.; Greber, T.; Hauke, F.; Hemmi, A.; Hernandez-Rodriguez, I.; Hirsch, A.; Hodge, S. A.; Huttel, Y.; Jepsen, P. U.; Jimenez, I.; Kaiser, U.; Kaplas, T.; Kim, H.; Kis, A.; Papagelis, K.; Kostarelos, K.; Krajewska, A.; Lee, K.; Li, C.; Lipsanen, H.; Liscio, A.; Lohe, M. R.; Loiseau, A.; Lombardi, L.; Francisca López, M.; Martin, O.; Martín, C.; Martínez, L.; Martin-Gago, J. A.; Ignacio Martínez, J.; Marzari, N.; Mayoral, Á.; McManus, J.; Melucci, M.; Méndez, J.; Merino, C.; Merino, P.; Meyer, A. P.; Miniussi, E.; Miseikis, V.; Mishra, N.; Morandi, V.; Munuera, C.; Muñoz, R.; Nolan, H.; Ortolani, L.; Ott, A. K.; Palacio, I.; Palermo, V.; Parthenios, J.; Pasternak, I.; Patane, A.; Prato, M.; Prevost, H.; Prudkovskiy, V.; Pugno, N.; Rojo, T.; Rossi, A.; Ruffieux, P.; Samorì, P.; Schué, L.; Setijadi, E.; Seyller, T.; Speranza, G.; Stampfer, C.; Stenger, I.; Strupinski, W.; Svirko, Y.; Taioli, S.; Teo, K. B. K.; Testi, M.; Tomarchio, F.; Tortello, M.; Treossi, E.; Turchanin, A.; Vazquez, E.; Villaro, E.; Whelan, P. R.; Xia, Z.; Yakimova, R.; Yang, S.; Yazdi, G. R.; Yim, C.; Yoon, D.; Zhang, X.; Zhuang, X.; Colombo, L.; Ferrari, A. C.; Garcia-Hernandez, M. Production and Processing of Graphene and Related Materials. *2D Mater.* **2020**, *7*, No. 022001.

(18) Karagiannidis, P. G.; Hodge, S. A.; Lombardi, L.; Tomarchio, F.; Decorde, N.; Milana, S.; Goykhman, I.; Su, Y.; Mesite, S. V.; Johnstone, D. N.; Leary, R. K.; Midgley, P. A.; Pugno, N. M.; Torrisi, F.; Ferrari, A. C. Microfluidization of Graphite and Formulation of Graphene-Based Conductive Inks. *ACS Nano* **2017**, *11*, 2742−2755.

(19) Hernandez, Y.; Nicolosi, V.; Lotya, M.; Blighe, F. M.; Sun, Z.; De, S.; McGovern, I. T.; Holland, B.; Byrne, M.; Gun'Ko, Y. K.; Boland, J. J.; Niraj, P.; Duesberg, G.; Krishnamurthy, S.; Goodhue, R.; Hutchison, J.; Scardaci, V.; Ferrari, A. C.; Coleman, J. N. High-Yield Production of Graphene by Liquid-Phase Exfoliation of Graphite. *Nat. Nanotechnol.* **2008**, *3*, 563−568.

(20) Ferrari, A. C.; Bonaccorso, F.; Fal'ko, V.; Novoselov, K. S.; Roche, S.; Bøggild, P.; Borini, S.; Koppens, F. H. L.; Palermo, V.; Pugno, N.; Garrido, J. A.; Sordan, R.; Bianco, A.; Ballerini, L.; Prato, M.; Lidorikis, E.; Kivioja, J.; Marinelli, C.; Ryhänen, T.; Morpurgo, A.; Coleman, J. N.; Nicolosi, V.; Colombo, L.; Fert, A.; Garcia-Hernandez, M.; Bachtold, A.; Schneider, G. F.; Guinea, F.; Dekker, C.; Barbone, M.; Sun, Z.; Galiotis, C.; Grigorenko, A. N.; Konstantatos, G.; Kis, A.; Katsnelson, M.; Vandersypen, L.; Loiseau, A.; Morandi, V.; Neumaier, D.; Treossi, E.; Pellegrini, V.; Polini, M.; Tredicucci, A.; Williams, G. M.; Hee Hong, B.; Ahn, J.-H.; Min Kim, J.; Zirath, H.; Van Wees, B. J.; Van Der Zant, H.; Occhipinti, L.; Di Matteo, A.; Kinloch, I. A.; Seyller, T.; Quesnel, E.; Feng, X.; Teo, K.; Rupesinghe, N.; Hakonen, P.; Neil, S. R. T.; Tannock, Q.; Löfwander, T.; Kinaret, J. Science and Technology Roadmap for Graphene, Related Two-Dimensional Crystals, and Hybrid Systems. *Nanoscale* **2015**, *7*, 4598−4810.

(21) Ji, L.; Rao, M.; Zheng, H.; Zhang, L.; Li, Y.; Duan, W.; Guo, J.; Cairns, E. J.; Zhang, Y. Graphene Oxide as a Sulfur Immobilizer in High Performance Lithium/Sulfur Cells. *J. Am. Chem. Soc.* **2011**, *133*, 18522−18525.

(22) Zhou, G.; Yin, L.-C.; Wang, D.-W.; Li, L.; Pei, S.; Gentle, I. R.; Li, F.; Cheng, H.-M. Fibrous Hybrid of Graphene and Sulfur Nanocrystals for High-Performance Lithium−Sulfur Batteries. *ACS Nano* **2013**, *7*, 5367−5375.

(23) Hou, T.-Z.; Chen, X.; Peng, H.-J.; Huang, J.-Q.; Li, B.-Q.; Zhang, Q.; Li, B. Design Principles for Heteroatom-Doped Nanocarbon to Achieve Strong Anchoring of Polysulfides for Lithium-Sulfur Batteries. *Small* **2016**, *12*, 3283−3291.

(24) Lochala, J.; Liu, D.; Wu, B.; Robinson, C.; Xiao, J. Research Progress toward the Practical Applications of Lithium−Sulfur Batteries. *ACS Appl. Mater. Interfaces* **2017**, *9*, 24407−24421.

(25) Doñoro, A.; Muñoz-Mauricio, Á.; Etacheri, V. High-Performance Lithium Sulfur Batteries Based on Multidimensional Graphene-CNT-Nanosulfur Hybrid Cathodes. *Batteries* **2021**, *7*, 26.

(26) Yang, C.; Li, P.; Yu, J.; Zhao, L.-D.; Kong, L. Approaching Energy-Dense and Cost-Effective Lithium−Sulfur Batteries: From Materials Chemistry and Price Considerations. *Energy* **2020**, *201*, No. 117718.

(27) Xi, K.; Kidambi, P. R.; Chen, R.; Gao, C.; Peng, X.; Ducati, C.; Hofmann, S.; Kumar, R. V. Binder Free Three-Dimensional Sulphur/Few-Layer Graphene Foam Cathode with Enhanced High-Rate Capability for Rechargeable Lithium Sulphur Batteries. *Nanoscale* **2014**, *6*, 5746−5753.

(28) Wu, P.; Sun, M.-H.; Yu, Y.; Peng, Z.; Bulbula, S. T.; Li, Y.; Chen, L.-H.; Su, B.-L. Physical and Chemical Dual-Confinement of Polysulfides within Hierarchically Meso-Microporous Nitrogen-Doped Carbon Nanocages for Advanced Li−S Batteries. *RSC Adv.* **2017**, *7*, 42627−42633.

(29) Liang, C.; Dudney, N. J.; Howe, J. Y. Hierarchically Structured Sulfur/Carbon Nanocomposite Material for High-Energy Lithium Battery. *Chem. Mater.* **2009**, *21*, 4724−4730.

(30) Guo, D.; Chen, X.; Wei, H.; Liu, M.; Ding, F.; Yang, Z.; Yang, K.; Wang, S.; Xu, X.; Huang, S. Controllable Synthesis of Highly Uniform Flower-like Hierarchical Carbon Nanospheres and Their Application in High Performance Lithium−Sulfur Batteries. *J. Mater. Chem. A* **2017**, *5*, 6245−6256.

(31) Zhao, X.; Kim, M.; Liu, Y.; Ahn, H.-J.; Kim, K.-W.; Cho, K.-K.; Ahn, J.-H. Root-like Porous Carbon Nanofibers with High Sulfur Loading Enabling Superior Areal Capacity of Lithium Sulfur Batteries. *Carbon* **2018**, *128*, 138−146.

(32) Zhang, S. S. Liquid Electrolyte Lithium/Sulfur Battery: Fundamental Chemistry, Problems, and Solutions. *J. Power Sources* **2013**, *231*, 153−162.

(33) Hu, G.; Xu, C.; Sun, Z.; Wang, S.; Cheng, H.; Li, F.; Ren, W. 3D Graphene-Foam−Reduced-Graphene-Oxide Hybrid Nested Hierarchical Networks for High-Performance Li−S Batteries. *Adv. Mater.* **2016**, *28*, 1603−1609.

(34) Jin, K.; Zhou, X.; Liu, Z. Graphene/Sulfur/Carbon Nanocomposite for High Performance Lithium-Sulfur Batteries. *Nanomaterials* **2015**, *5*, 1481−1492.

(35) Wang, H.; Yang, Y.; Liang, Y.; Robinson, J. T.; Li, Y.; Jackson, A.; Cui, Y.; Dai, H. Graphene-Wrapped Sulfur Particles as a Rechargeable Lithium−Sulfur Battery Cathode Material with High Capacity and Cycling Stability. *Nano Lett.* **2011**, *11*, 2644−2647.

(36) Yuan, S.; Guo, Z.; Wang, L.; Hu, S.; Wang, Y.; Xia, Y. Leaf-Like Graphene-Oxide-Wrapped Sulfur for High-Performance Lithium−Sulfur Battery. *Adv. Sci.* **2015**, *2*, No. 1500071.

(37) Qiu, Y.; Li, W.; Zhao, W.; Li, G.; Hou, Y.; Liu, M.; Zhou, L.; Ye, F.; Li, H.; Wei, Z.; Yang, S.; Duan, W.; Ye, Y.; Guo, J.; Zhang, Y. High-Rate, Ultralong Cycle-Life Lithium/Sulfur Batteries Enabled by Nitrogen-Doped Graphene. *Nano Lett.* **2014**, *14*, 4821−4827.

(38) Du, Z.; Xu, J.; Jin, S.; Shi, Y.; Guo, C.; Kong, X.; Zhu, Y.; Ji, H. The Correlation between Carbon Structures and Electrochemical Properties of Sulfur/Carbon Composites for Li-S Batteries. *J. Power Sources* **2017**, *341*, 139−146.

(39) Li, M.; Hu, P.; Wang, X.; Niu, Z.; Zhou, Q.; Wang, Q.; Zhu, M.; Guo, C.; Zhang, L.; Lu, J.; Li, J. Hierarchical Porous Carbon Derived from Peanut Hull for Polysulfide Confinement in Lithium−Sulfur Batteries. *Energy Technol.* **2019**, *7*, No. 1800898.

(40) Yang, X.; Zhang, L.; Zhang, F.; Huang, Y.; Chen, Y. Sulfur-Infiltrated Graphene-Based Layered Porous Carbon Cathodes for High-Performance Lithium−Sulfur Batteries. *ACS Nano* **2014**, *8*, 5208−5215.

(41) Cao, Y.; Li, X.; Aksay, I. A.; Lemmon, J.; Nie, Z.; Yang, Z.; Liu, J. Sandwich-Type Functionalized Graphene Sheet-Sulfur Nanocomposite for Rechargeable Lithium Batteries. *Phys. Chem. Chem. Phys.* **2011**, *13*, 7660.

(42) Guo, J.; Xu, Y.; Wang, C. Sulfur-Impregnated Disordered Carbon Nanotubes Cathode for Lithium−Sulfur Batteries. *Nano Lett.* **2011**, *11*, 4288−4294.

(43) Cheng, D.; Zhao, Y.; An, T.; Wang, X.; Zhou, H.; Fan, T. 3D Interconnected Crumpled Porous Carbon Sheets Modified with High-Level Nitrogen Doping for High Performance Lithium Sulfur Batteries. *Carbon* **2019**, *154*, 58−66.

https://doi.org/10.1021/acsmaterialslett.4c01646
ACS Materials Lett. 2024, 6, 5363−5374

(44) Zhou, Z.; Wang, Z.; Ji, J.; Fu, K.; Cao, C.; Yang, J.; Xue, Y.; Tang, C. Uniform Embedding of Ultrafine Sulfur into Well-Honeycombed Porous Graphene Frameworks for Highly Stable Li−S Batteries. *Mater. Lett.* **2020**, *276*, No. 128243.
(45) Li, Y.; Cai, Y.; Cai, Z.; Xu, J.; Sonamuthu, J.; Zhu, G.; Militky, J.; Jin, W.; Yao, J. Sulfur-Infiltrated Yeast-Derived Nitrogen-Rich Porous Carbon Microspheres @ Reduced Graphene Cathode for High-Performance Lithium-Sulfur Batteries. *Electrochim. Acta* **2018**, *285*, 317−325.
(46) Zhou, X.; Ma, X.; Ding, C.; Meng, W.; Xu, S.; Chen, L.; Duan, D.; Liu, S. A 3D Stable and Highly Conductive Scaffold with Carbon Nanotubes/Carbon Fiber as Electrode for Lithium Sulfur Batteries. *Mater. Lett.* **2019**, *251*, 180−183.
(47) Lin, T.; Tang, Y.; Wang, Y.; Bi, H.; Liu, Z.; Huang, F.; Xie, X.; Jiang, M. Scotch-Tape-like Exfoliation of Graphite Assisted with Elemental Sulfur and Graphene−Sulfur Composites for High-Performance Lithium-Sulfur Batteries. *Energy Environ. Sci.* **2013**, *6*, 1283.
(48) Xu, G.; Yuan, J.; Geng, X.; Dou, H.; Chen, L.; Yan, X.; Zhu, H. Caterpillar-like Graphene Confining Sulfur by Restacking Effect for High Performance Lithium Sulfur Batteries. *Chem. Eng. J.* **2017**, *322*, 454−462.
(49) Zheng, G.; Yang, Y.; Cha, J. J.; Hong, S. S.; Cui, Y. Hollow Carbon Nanofiber-Encapsulated Sulfur Cathodes for High Specific Capacity Rechargeable Lithium Batteries. *Nano Lett.* **2011**, *11*, 4462−4467.
(50) Tukamoto, H.; West, A. R. Electronic Conductivity of LiCoO2 and Its Enhancement by Magnesium Doping. *J. Electrochem. Soc.* **1997**, *144*, 3164−3168.
(51) Padhi, A. K.; Nanjundaswamy, K. S.; Goodenough, J. B. Phospho-olivines as Positive-Electrode Materials for Rechargeable Lithium Batteries. *J. Electrochem. Soc.* **1997**, *144*, 1188−1194.
(52) Chung, S.-Y.; Bloking, J. T.; Chiang, Y.-M. Electronically Conductive Phospho-Olivines as Lithium Storage Electrodes. *Nat. Mater.* **2002**, *1*, 123−128.
(53) Liu, G.; Zheng, H.; Simens, A. S.; Minor, A. M.; Song, X.; Battaglia, V. S. Optimization of Acetylene Black Conductive Additive and PVDF Composition for High-Power Rechargeable Lithium-Ion Cells. *J. Electrochem. Soc.* **2007**, *154*, A1129.
(54) Liu, G.; Zheng, H.; Kim, S.; Deng, Y.; Minor, A. M.; Song, X.; Battaglia, V. S. Effects of Various Conductive Additive and Polymeric Binder Contents on the Performance of a Lithium-Ion Composite Cathode. *J. Electrochem. Soc.* **2008**, *155*, A887.
(55) Al-Mahmoud, S. M.; Dibden, J. W.; Owen, J. R.; Denuault, G.; Garcia-Araez, N. A Simple, Experiment-Based Model of the Initial Self-Discharge of Lithium-Sulphur Batteries. *J. Power Sources* **2016**, *306*, 323−328.
(56) Bhargav, A.; He, J.; Gupta, A.; Manthiram, A. Lithium-Sulfur Batteries: Attaining the Critical Metrics. *Joule* **2020**, *4*, 285−291.
(57) Lacey, M. J.; Jeschull, F.; Edström, K.; Brandell, D. Porosity Blocking in Highly Porous Carbon Black by PVdF Binder and Its Implications for the Li−S System. *J. Phys. Chem. C* **2014**, *118*, 25890−25898.
(58) Chen, S.-R.; Zhai, Y.-P.; Xu, G.-L.; Jiang, Y.-X.; Zhao, D.-Y.; Li, J.-T.; Huang, L.; Sun, S.-G. Ordered Mesoporous Carbon/Sulfur Nanocomposite of High Performances as Cathode for Lithium−Sulfur Battery. *Electrochim. Acta* **2011**, *56*, 9549−9555.
(59) Yan, X.; Zhang, H.; Huang, M.; Jia, W.; Jiang, Y.; Chen, T.; Qu, M. Micro/Nano-Structure Construct of Carbon Fibers Reinforced Graphene/CNT Matrix Composites for Li-S Batteries. *Diam. Relat. Mater.* **2022**, *123*, No. 108888.
(60) Wu, Y.; Xu, C.; Guo, J.; Su, Q.; Du, G.; Zhang, J. Enhanced Electrochemical Performance by Wrapping Graphene on Carbon Nanotube/Sulfur Composites for Rechargeable Lithium−Sulfur Batteries. *Mater. Lett.* **2014**, *137*, 277−280.
(61) Schneider, A.; Janek, J.; Brezesinski, T. Improving the Capacity of Lithium−Sulfur Batteries by Tailoring the Polysulfide Adsorption Efficiency of Hierarchical Oxygen/Nitrogen-Functionalized Carbon Host Materials. *Phys. Chem. Chem. Phys.* **2017**, *19*, 8349−8355.
(62) Gómez-Urbano, J. L.; Gómez-Cámer, J. L.; Botas, C.; Rojo, T.; Carriazo, D. Graphene Oxide-Carbon Nanotubes Aerogels with High Sulfur Loadings Suitable as Binder-Free Cathodes for High Performance Lithium Sulfur Batteries. *J. Power Sources* **2019**, *412*, 408−415.
(63) Wei, B.; Shang, C.; Pan, X.; Chen, Z.; Shui, L.; Wang, X.; Zhou, G. Lotus Root-Like Nitrogen-Doped Carbon Nanofiber Structure Assembled with VN Catalysts as a Multifunctional Host for Superior Lithium−Sulfur Batteries. *Nanomaterials* **2019**, *9*, 1724.
(64) Fransson, L.; Eriksson, T.; Edstrom, K.; Gustafsson, T.; Thomas, J. O. Influence of Carbon Black and Binder on Li-Ion Batteries. *J. Power Sources* **2001**, *101*, 1−9.
(65) Pasquier, A. D.; Disma, F.; Bowmer, T.; Gozdz, A. S.; Amatucci, G.; Tarascon, J.-M. Differential Scanning Calorimetry Study of the Reactivity of Carbon Anodes in Plastic Li-Ion Batteries. *J. Electrochem. Soc.* **1998**, *145*, 472−477.
(66) Hencz, L.; Chen, H.; Ling, H. Y.; Wang, Y.; Lai, C.; Zhao, H.; Zhang, S. Housing Sulfur in Polymer Composite Frameworks for Li−S Batteries. *Nano-Micro Lett.* **2019**, *11*, 17.
(67) Guo, R.; Yang, Y.; Huang, X. L.; Zhao, C.; Hu, B.; Huo, F.; Liu, H. K.; Sun, B.; Sun, Z.; Dou, S. X. Recent Advances in Multifunctional Binders for High Sulfur Loading Lithium-Sulfur Batteries. *Adv. Funct. Mater.* **2024**, *34*, No. 2307108.
(68) Zhao, Y.; Liang, Z.; Kang, Y.; Zhou, Y.; Li, Y.; He, X.; Wang, L.; Mai, W.; Wang, X.; Zhou, G.; Wang, J.; Li, J.; Tavajohi, N.; Li, B. Rational Design of Functional Binder Systems for High-Energy Lithium-Based Rechargeable Batteries. *Energy Storage Mater.* **2021**, *35*, 353−377.
(69) Shaibani, M.; Mirshekarloo, M. S.; Singh, R.; Easton, C. D.; Cooray, M. C. D.; Eshraghi, N.; Abendroth, T.; Dörfler, S.; Althues, H.; Kaskel, S.; Hollenkamp, A. F.; Hill, M. R.; Majumder, M. Expansion-Tolerant Architectures for Stable Cycling of Ultrahigh-Loading Sulfur Cathodes in Lithium-Sulfur Batteries. *Sci. Adv.* **2020**, *6*, No. eaay2757.
(70) Dou, W.; Zheng, M.; Zhang, W.; Liu, T.; Wang, F.; Wan, G.; Liu, Y.; Tao, X. Review on the Binders for Sustainable High-Energy-Density Lithium Ion Batteries: Status, Solutions, and Prospects. *Adv. Funct. Mater.* **2023**, *33*, No. 2305161.
(71) Aurbach, D.; Pollak, E.; Elazari, R.; Salitra, G.; Kelley, C. S.; Affinito, J. On the Surface Chemical Aspects of Very High Energy Density, Rechargeable Li−Sulfur Batteries. *J. Electrochem. Soc.* **2009**, *156*, A694.
(72) Zhang, L.; Ling, M.; Feng, J.; Mai, L.; Liu, G.; Guo, J. The Synergetic Interaction between LiNO3 and Lithium Polysulfides for Suppressing Shuttle Effect of Lithium-Sulfur Batteries. *Energy Storage Mater.* **2018**, *11*, 24−29.
(73) Agostini, M.; Hwang, J.; Kim, H. M.; Bruni, P.; Brutti, S.; Croce, F.; Matic, A.; Sun, Y. Minimizing the Electrolyte Volume in Li−S Batteries: A Step Forward to High Gravimetric Energy Density. *Adv. Energy Mater.* **2018**, *8*, No. 1801560.
(74) Zhang, S. S. Role of LiNO3 in Rechargeable Lithium/Sulfur Battery. *Electrochim. Acta* **2012**, *70*, 344−348.
(75) Liang, X.; Wen, Z.; Liu, Y.; Wu, M.; Jin, J.; Zhang, H.; Wu, X. Improved Cycling Performances of Lithium Sulfur Batteries with LiNO3-Modified Electrolyte. *J. Power Sources* **2011**, *196*, 9839−9843.
(76) United Nations. *Recommendations on the Transport of Dangerous Goods—Manual of Tests and Criteria.*; United Nations: New York, 2015. Available via the Internet at: https://web.archive.org/web/20230514213432/https%3A%2F%2Funece.org%2Ffileadmin%2FDAM%2Ftrans%2Fdanger%2FST_SG_AC.10_11_Rev6_E_WEB_-With_corrections_from_Corr.1.pdf accessed June 2, 2023.
(77) Zhang, S. S. Effect of Discharge Cutoff Voltage on Reversibility of Lithium/Sulfur Batteries with $LiNO_3$-Contained Electrolyte. *J. Electrochem. Soc.* **2012**, *159*, A920−A923.
(78) Hettesheimer, T.; Neef, C.; Rosellón Inclán, I.; Link, S.; Schmaltz, T.; Schuckert, F.; Stephan, A.; Stephan, M.; Thielmann, A.; Weymann, L.; Wicke, T. *Lithium-Ion Battery Roadmap—Industrialization Perspectives toward 2030*; Fraunhofer ISI, 2023, DOI: 10.24406/PUBLICA-2153.

https://doi.org/10.1021/acsmaterialslett.4c01646
ACS Materials Lett. 2024, 6, 5363−5374

(79) Mikhaylik, Y. V.; Akridge, J. R. Polysulfide Shuttle Study in the Li/S Battery System. *J. Electrochem. Soc.* **2004**, *151*, A1969.
(80) Zheng, J.; Gu, M.; Wagner, M. J.; Hays, K. A.; Li, X.; Zuo, P.; Wang, C.; Zhang, J.-G.; Liu, J.; Xiao, J. Revisit Carbon/Sulfur Composite for Li-S Batteries. *J. Electrochem. Soc.* **2013**, *160*, A1624−A1628.
(81) Di Lecce, D.; Marangon, V.; Du, W.; Brett, D. J. L.; Shearing, P. R.; Hassoun, J. The Role of Synthesis Pathway on the Microstructural Characteristics of Sulfur-Carbon Composites: X-Ray Imaging and Electrochemistry in Lithium Battery. *J. Power Sources* **2020**, *472*, No. 228424.
(82) Neubauer, J.; Pesaran, A.; Bae, C.; Elder, R.; Cunningham, B. Updating United States Advanced Battery Consortium and Department of Energy Battery Technology Targets for Battery Electric Vehicles. *J. Power Sources* **2014**, *271*, 614−621.
(83) Wang, Z.; Xue, D.; Song, H.; Zhong, X.; Wang, J.; Hou, P. Hierarchical Micro-Mesoporous Carbon Prepared from Waste Cotton Textile for Lithium-Sulfur Batteries. *Ionics* **2019**, *25*, 4057−4066.
(84) Tan, C.; Heenan, T. M. M.; Ziesche, R. F.; Daemi, S. R.; Hack, J.; Maier, M.; Marathe, S.; Rau, C.; Brett, D. J. L.; Shearing, P. R. Four-Dimensional Studies of Morphology Evolution in Lithium−Sulfur Batteries. *ACS Appl. Energy Mater.* **2018**, *1*, 5090−5100.
(85) Lyu, Z.; Xu, D.; Yang, L.; Che, R.; Feng, R.; Zhao, J.; Li, Y.; Wu, Q.; Wang, X.; Hu, Z. Hierarchical Carbon Nanocages Confining High-Loading Sulfur for High-Rate Lithium−Sulfur Batteries. *Nano Energy* **2015**, *12*, 657−665.
(86) Yu, L.; Brun, N.; Sakaushi, K.; Eckert, J.; Titirici, M. M. Hydrothermal Nanocasting: Synthesis of Hierarchically Porous Carbon Monoliths and Their Application in Lithium−Sulfur Batteries. *Carbon* **2013**, *61*, 245−253.
(87) Zhao, M.-Q.; Zhang, Q.; Huang, J.-Q.; Tian, G.-L.; Nie, J.-Q.; Peng, H.-J.; Wei, F. Unstacked Double-Layer Templated Graphene for High-Rate Lithium−Sulphur Batteries. *Nat. Commun.* **2014**, *5*, 3410.
(88) Zhou, G.; Li, L.; Ma, C.; Wang, S.; Shi, Y.; Koratkar, N.; Ren, W.; Li, F.; Cheng, H.-M. A Graphene Foam Electrode with High Sulfur Loading for Flexible and High Energy Li-S Batteries. *Nano Energy* **2015**, *11*, 356−365.
(89) Zhou, G.; Pei, S.; Li, L.; Wang, D.; Wang, S.; Huang, K.; Yin, L.; Li, F.; Cheng, H. A Graphene−Pure-Sulfur Sandwich Structure for Ultrafast, Long-Life Lithium−Sulfur Batteries. *Adv. Mater.* **2014**, *26*, 625−631.
(90) Bao, W.; Zhang, Z.; Chen, W.; Zhou, C.; Lai, Y.; Li, J. Facile Synthesis of Graphene Oxide @ Mesoporous Carbon Hybrid Nanocomposites for Lithium Sulfur Battery. *Electrochim. Acta* **2014**, *127*, 342−348.
(91) Carbone, L.; Del Rio Castillo, A. E.; Kumar Panda, J.; Pugliese, G.; Scarpellini, A.; Bonaccorso, F.; Pellegrini, V. High-Sulfur-Content Graphene-Based Composite through Ethanol Evaporation for High-Energy Lithium-Sulfur Battery. *ChemSusChem* **2020**, *13*, 1593−1602.
(92) Chen, M.; Su, Z.; Jiang, K.; Pan, Y.; Zhang, Y.; Long, D. Promoting Sulfur Immobilization by a Hierarchical Morphology of Hollow Carbon Nanosphere Clusters for High-Stability Li−S Battery. *J. Mater. Chem. A* **2019**, *7*, 6250−6258.
(93) Choudhury, S.; Ebert, T.; Windberg, T.; Seifert, A.; Göbel, M.; Simon, F.; Formanek, P.; Stamm, M.; Spange, S.; Ionov, L. Hierarchical Porous Carbon Cathode for Lithium−Sulfur Batteries Using Carbon Derived from Hybrid Materials Synthesized by Twin Polymerization. *Part. Part. Syst. Charact.* **2018**, *35*, No. 1800364.
(94) Guo, J.; Zhang, J.; Jiang, F.; Zhao, S.; Su, Q.; Du, G. Microporous Carbon Nanosheets Derived from Corncobs for Lithium−Sulfur Batteries. *Electrochim. Acta* **2015**, *176*, 853−860.
(95) Han, P.; Chung, S.; Manthiram, A. Pyrrolic-Type Nitrogen-Doped Hierarchical Macro/Mesoporous Carbon as a Bifunctional Host for High-Performance Thick Cathodes for Lithium-Sulfur Batteries. *Small* **2019**, *15*, No. 1900690.
(96) Huang, J.-Q.; Liu, X.-F.; Zhang, Q.; Chen, C.-M.; Zhao, M.-Q.; Zhang, S.-M.; Zhu, W.; Qian, W.-Z.; Wei, F. Entrapment of Sulfur in Hierarchical Porous Graphene for Lithium−Sulfur Batteries with High Rate Performance from − 40 to 60°C. *Nano Energy* **2013**, *2*, 314−321.
(97) Jayaprakash, N.; Shen, J.; Moganty, S. S.; Corona, A.; Archer, L. A. Porous Hollow Carbon@Sulfur Composites for High-Power Lithium−Sulfur Batteries. *Angew. Chem., Int. Ed.* **2011**, *50*, 5904−5908.
(98) Kalaiappan, K.; Marimuthu, S.; Rengapillai, S.; Murugan, R.; Premkumar, T. Kombucha Scoby-Based Carbon as a Green Scaffold for High-Capacity Cathode in Lithium−Sulfur Batteries. *Ionics* **2019**, *25*, 4637−4650.
(99) Liu, S.; Zhao, T.; Tan, X.; Guo, L.; Wu, J.; Kang, X.; Wang, H.; Sun, L.; Chu, W. 3D Pomegranate-like Structures of Porous Carbon Microspheres Self-Assembled by Hollow Thin-Walled Highly-Graphitized Nanoballs as Sulfur Immobilizers for Li−S Batteries. *Nano Energy* **2019**, *63*, No. 103894.
(100) Liu, S.; Xie, K.; Li, Y.; Chen, Z.; Hong, X.; Zhou, L.; Yuan, J.; Zheng, C. Graphene Oxide Wrapped Hierarchical Porous Carbon−Sulfur Composite Cathode with Enhanced Cycling and Rate Performance for Lithium Sulfur Batteries. *RSC Adv.* **2015**, *5*, 5516−5522.
(101) Luo, C.; Niu, S.; Zhou, G.; Lv, W.; Li, B.; Kang, F.; Yang, Q.-H. Dual-Functional Hard Template Directed One-Step Formation of a Hierarchical Porous Carbon−Carbon Nanotube Hybrid for Lithium−Sulfur Batteries. *Chem. Commun.* **2016**, *52*, 12143−12146.
(102) Qiu, Y.; Wu, X.; Wang, M.; Fan, L.; Tian, D.; Guan, B.; Tang, D.; Zhang, N. 3D Hierarchical CNT-Based Host with High Sulfur Loading for Lithium-Sulfur Batteries. *ChemElectroChem.* **2019**, *6*, 5698−5704.
(103) Qu, Y.; Zhang, Z.; Zhang, X.; Ren, G.; Wang, X.; Lai, Y.; Liu, Y.; Li, J. Synthesis of Hierarchical Porous Honeycomb Carbon for Lithium-Sulfur Battery Cathode with High Rate Capability and Long Cycling Stability. *Electrochim. Acta* **2014**, *137*, 439−446.
(104) Tang, C.; Li, B.; Zhang, Q.; Zhu, L.; Wang, H.; Shi, J.; Wei, F. CaO-Templated Growth of Hierarchical Porous Graphene for High-Power Lithium−Sulfur Battery Applications. *Adv. Funct. Mater.* **2016**, *26*, 577−585.
(105) Wang, M.; Zhang, H.; Zhou, W.; Yang, X.; Li, X.; Zhang, H. Rational Design of a Nested Pore Structure Sulfur Host for Fast Li/S Batteries with a Long Cycle Life. *J. Mater. Chem. A* **2016**, *4*, 1653−1662.
(106) Wang, N.; Wang, J.; Zhao, J.; Wang, J.; Pan, J.; Huang, J. Synthesis of Porous-Carbon@reduced Graphene Oxide with Superior Electrochemical Behaviors for Lithium-Sulfur Batteries. *J. Alloys Compd.* **2021**, *851*, No. 156832.
(107) Wu, F.; Zhao, S.; Chen, L.; Lu, Y.; Su, Y.; Li, J.; Bao, L.; Yao, J.; Zhou, Y.; Chen, R. Electron Bridging Structure Glued Yolk-Shell Hierarchical Porous Carbon/Sulfur Composite for High Performance Li-S Batteries. *Electrochim. Acta* **2018**, *292*, 199−207.
(108) Wu, H.; Xia, L.; Ren, J.; Zheng, Q.; Xie, F.; Jie, W.; Xu, C.; Lin, D. A Multidimensional and Nitrogen-Doped Graphene/Hierarchical Porous Carbon as a Sulfur Scaffold for High Performance Lithium Sulfur Batteries. *Electrochim. Acta* **2018**, *278*, 83−92.
(109) Yang, W.; Yang, W.; Song, A.; Sun, G.; Shao, G. 3D Interconnected Porous Carbon Nanosheets/Carbon Nanotubes as a Polysulfide Reservoir for High Performance Lithium−Sulfur Batteries. *Nanoscale* **2018**, *10*, 816−824.
(110) Zhang, Y.; Duan, X.; Wang, J.; Wang, C.; Wang, J.; Wang, J.; Wang, J. Natural Graphene Microsheets/Sulfur as Li-S Battery Cathode towards > 99% Coulombic Efficiency of Long Cycles. *J. Power Sources* **2018**, *376*, 131−137.
(111) Zhang, Y.; Sun, K.; Liang, Z.; Wang, Y.; Ling, L. N-Doped Yolk-Shell Hollow Carbon Sphere Wrapped with Graphene as Sulfur Host for High-Performance Lithium-Sulfur Batteries. *Appl. Surf. Sci.* **2018**, *427*, 823−829.
(112) Benítez, A.; Caballero, A.; Morales, J.; Hassoun, J.; Rodríguez-Castellón, E.; Canales-Vázquez, J. Physical Activation of Graphene: An Effective, Simple and Clean Procedure for Obtaining Microporous Graphene for High-Performance Li/S Batteries. *Nano Res.* **2019**, *12*, 759−766.

https://doi.org/10.1021/acsmaterialslett.4c01646
ACS Materials Lett. 2024, 6, 5363−5374

(113) Han, W.; Li, Q.; Zhu, H.; Luo, D.; Qin, X.; Li, B. Hierarchical Porous Graphene Bubbles as Host Materials for Advanced Lithium Sulfur Battery Cathode. *Front. Chem.* **2021**, *9*, No. 653476.
(114) Li, H.; Sun, L.; Zhao, Y.; Tan, T.; Zhang, Y. Blackberry-like Hollow Graphene Spheres Synthesized by Spray Drying for High-Performance Lithium-Sulfur Batteries. *Electrochim. Acta* **2019**, *295*, 822−828.
(115) Niu, S.; Wu, S.; Lu, W.; Yang, Q.; Kang, F. A One-Step Hard-Templating Method for the Preparation of a Hierarchical Micro-porous-Mesoporous Carbon for Lithium-Sulfur Batteries. *New Carbon Mater.* **2017**, *32*, 289−296.
(116) Qian, W.; Gao, Q.; Yang, K.; Tian, W.; Tan, Y.; Yang, C.; Zhang, H.; Li, Z.; Zhu, L. 3D Hierarchically Interconnected Porous Graphene Containing Sulfur for Stable High Rate Li−S Batteries. *Energy Technol.* **2016**, *4*, 625−632.
(117) Tian, T.; Li, B.; Zhu, M.; Liu, J.; Li, S. Sandwich-like Graphene-Mesoporous Carbon as Sulfur Host for Enhanced Lithium−Sulfur Batteries. *Mater. Res. Express* **2017**, *4*, No. 105017.
(118) Wu, F.; Shi, L.; Mu, D.; Xu, H.; Wu, B. A Hierarchical Carbon Fiber/Sulfur Composite as Cathode Material for Li−S Batteries. *Carbon* **2015**, *86*, 146−155.
(119) Thommes, M.; Kaneko, K.; Neimark, A. V.; Olivier, J. P.; Rodriguez-Reinoso, F.; Rouquerol, J.; Sing, K. S. W. Physisorption of Gases, with Special Reference to the Evaluation of Surface Area and Pore Size Distribution (IUPAC Technical Report). *Pure Appl. Chem.* **2015**, *87*, 1051−1069.
(120) Sun, Y.-K. An Experimental Checklist for Reporting Battery Performances. *ACS Energy Lett.* **2021**, *6*, 2187−2189.
(121) Stephan, A. K. Standardized Battery Reporting Guidelines. *Joule* **2021**, *5*, 1−2.
(122) Li, J.; Arbizzani, C.; Kjelstrup, S.; Xiao, J.; Xia, Y.; Yu, Y.; Yang, Y.; Belharouak, I.; Zawodzinski, T.; Myung, S.-T.; Raccichini, R.; Passerini, S. Good Practice Guide for Papers on Batteries for the Journal of Power Sources. *J. Power Sources* **2020**, *452*, No. 227824.

https://doi.org/10.1021/acsmaterialslett.4c01646
ACS Materials Lett. 2024, 6, 5363−5374